

# Microwave conductivity of $\text{YBa}_2\text{Cu}_3\text{O}_{6.99}$ including inelastic scattering

E. Schachinger<sup>1</sup> and J. P. Carbotte<sup>2</sup><sup>1</sup>*Institut für Theoretische Physik, Technische Universität Graz, A-8010 Graz, Austria*<sup>2</sup>*Department of Physics and Astronomy, McMaster University, Hamilton, Ontario, Canada L8S 4M1*

(Received 20 August 2001; published 17 January 2002)

The fluctuation spectrum responsible for the inelastic scattering in  $\text{YBa}_2\text{Cu}_3\text{O}_{6.99}$ , which was recently determined from consideration of the in-plane optical conductivity in the infrared, is used to calculate the temperature dependence of the microwave conductivity at several measured frequencies. Reasonable overall agreement can only be achieved if, in addition, some impurity scattering is included within a model potential intermediate between weak (Born) and strong (unitary) limit.

DOI: 10.1103/PhysRevB.65.064514

PACS number(s): 74.20.Mn, 74.25.Gz, 74.72.-h

## I. INTRODUCTION

In a recent paper Carbotte *et al.*<sup>1</sup> showed that the 41 meV spin resonance observed in spin-polarized neutron scattering experiments<sup>2</sup> on  $\text{YBa}_2\text{Cu}_3\text{O}_{6.95}$  (YBCO) has a counterpart in the infrared optical conductivity in which an optical resonance is seen at the same energy demonstrating its coupling to the charge carriers.<sup>3,4</sup> The temperature evolution of the spin resonance can be determined from consideration of the frequency dependence of the optical scattering rate measured at several different temperatures<sup>5</sup> in the superconducting state. The required analysis which allows one to extract the resonance from the optics is carried out within a generalized Eliashberg formalism for a *d*-wave superconductor.<sup>6</sup> The end result is a charge-carrier-exchange boson excitation spectral density which characterizes the inelastic scattering. The spectral density  $I^2\chi(\omega)$  shows a distinct evolution with decreasing temperature. At  $T_c$  the spectrum obtained is linear in  $\omega$  at small  $\omega$ , followed by a broad peak at some characteristic energy  $\omega_{SF}$ , and then there is a very slow decay at higher  $\omega$  extending up to a cutoff  $\omega_c$  of order 400 meV. This spectrum can be fit with the spin fluctuation form employed in Pines' group,<sup>7,8</sup>

$$I^2 \frac{\omega/\omega_{SF}}{1 + (\omega/\omega_{SF})^2} \theta(\omega_c - \omega)$$

[Millis-Monien-Pines (MMP) model], where  $I^2$  is a coupling constant to the charge carriers. As the temperature is lowered below  $T_c$ , the fluctuation spectrum obtained from the infrared data undergoes important changes. It develops a gap at the lowest energies as well as a peak at 41 meV. The strength of this peak tracks well the observed growth of the area under the spin susceptibility,  $\text{Im}\{\chi(\mathbf{q}, \omega)\}$ , at  $\mathbf{q}=(\pi, \pi)$ , measured by Dai *et al.*<sup>9</sup> in neutron scattering. The higher-energy part, however, remains largely unaffected. The observed changes in spectral density are as expected and are interpreted as coming from feedback effects on the excitation spectrum due to the changes brought about in the electronic system by the onset of superconductivity. This arises in any purely electronic mechanism of superconductivity in which the pairing proceeds through bosons exchanged between the charge carriers and where the bosons themselves are intrinsic to the electronic system.<sup>6,10</sup> The changes in the low-energy

part of  $I^2\chi(\omega)$  lead directly to the phenomenon referred to as the collapse of the quasiparticle scattering rate and are responsible for the freezing out of the inelastic scattering at low temperatures. In turn, this leads to a prominent peak around 30 K in the in-plane microwave conductivity<sup>11</sup> as a function of temperature  $T$  and a corresponding peak in the electronic thermal conductivity.<sup>12</sup>

Schachinger *et al.*<sup>5</sup> have recently found that this same spectral density  $I^2\chi(\omega)$  also gives, within an Eliashberg formalism, good agreement with observed properties of the superconducting state such as the ratio of the gap to the critical temperature, the fractional optical spectral weight involved in the condensation (superfluid stiffness), the temperature dependence of the penetration depth, and the magnitude of the condensation energy, as well as other quantities. It is also obvious from the way the temperature-dependent spectral density has been derived in Ref. 5 that the coupling to the 41 meV spin resonance in YBCO cannot play the role of the "glue" leading to superconductivity<sup>13</sup> because it is absent at  $T_c$ .

In this paper we consider the temperature dependence of the microwave conductivity for five different frequencies between 1 and 75 GHz observed recently<sup>14</sup> in ultrapure samples of  $\text{YBa}_2\text{Cu}_3\text{O}_{6.99}$  grown in  $\text{BaZnO}_3$  crucibles. Our calculations are based on the previously determined spectral density  $I^2\chi(\omega)$  for twinned YBCO single crystals which is not modified in any way. It is found, however, that to understand the low-temperature data (10–20 K) it is necessary to additionally introduce some elastic impurity scattering. A model impurity potential intermediate between weak (Born) and strong (unitary) scattering is developed which provides a reasonable, if not perfect overall fit to the data.

In Sec. II we give the necessary formalism. This is followed by the presentation of our results in Sec. III. Comparison with the data is also presented in this section. Section IV contains discussion and a conclusion.

## II. FORMALISM

We consider a *d*-wave superconductor. To include the inelastic scattering which is known to be strong in the cuprates we need to go beyond a simple BCS formalism. The minimum set of equations that allows us to do this are generalized Eliashberg equations. These equations involve two

channels. The ordinary renormalization channel which remains in the normal state and leads to renormalization of the Matsubara frequencies by the interactions. The second is the pairing channel which we assume to have  $d$ -wave character. For simplicity we take the pairing potential to be separable in incoming ( $\mathbf{k}$ ) and outgoing ( $\mathbf{k}'$ ) momenta in the two-dimensional  $\text{CuO}_2$  Brillouin zone. The charge-carrier-fluctuation spectrum spectral density  $I^2\chi(\omega)$  which characterizes the inelastic scattering in the renormalization channel is assumed to also cause the pairing and while, in principle, the spectral density could have a different shape in this case, for simplicity we ignore such complications. We do allow, however, for a possible difference in magnitude through a constant  $g$ . For the renormalized frequencies  $\tilde{\omega}$  we use  $I^2\chi(\omega)$  and  $\tilde{\omega}(\omega+i\delta)$  as isotropic while for the pairing energy  $\tilde{\Delta}$  we use  $gI^2\chi(\omega)\cos(2\phi)\cos(2\phi')$  which immediately leads to a  $d$ -wave form  $\tilde{\Delta}(\omega+i\delta)\sim\cos(2\phi)$ , where  $\phi$  is the angle defining the direction of momentum  $\mathbf{k}$  on a cylindrical Fermi surface.

The generalized Eliashberg equations which play the central role in this study are

$$\begin{aligned} \tilde{\Delta}(\nu+i\delta;\phi) &= \pi T g \sum_{m=0}^{\infty} \cos(2\phi) [\lambda(\nu-i\omega_m) + \lambda(\nu+i\omega_m)] \\ &\times \left\langle \frac{\tilde{\Delta}(i\omega_m;\phi') \cos(2\phi')}{\sqrt{\tilde{\omega}^2(i\omega_m) + \tilde{\Delta}^2(i\omega_m;\phi')}} \right\rangle' + i\pi g \\ &\times \int_{-\infty}^{\infty} dz \cos(2\phi) I^2\chi(z) [n(z) + f(z-\nu)] \\ &\times \left\langle \frac{\tilde{\Delta}(\nu-z+i\delta;\phi') \cos(2\phi')}{\sqrt{\tilde{\omega}^2(\nu-z+i\delta) - \tilde{\Delta}^2(\nu-z+i\delta;\phi')}} \right\rangle' \end{aligned} \quad (1a)$$

and, in the renormalization channel,

$$\begin{aligned} \tilde{\omega}(\nu+i\delta) &= \nu + i\pi T \sum_{m=0}^{\infty} [\lambda(\nu-i\omega_m) - \lambda(\nu+i\omega_m)] \\ &\times \left\langle \frac{\tilde{\omega}(i\omega_m)}{\sqrt{\tilde{\omega}^2(i\omega_m) + \tilde{\Delta}^2(i\omega_m;\phi')}} \right\rangle' \\ &+ i\pi \int_{-\infty}^{\infty} dz I^2\chi(z) [n(z) + f(z-\nu)] \\ &\times \left\langle \frac{\tilde{\omega}(\nu-z+i\delta)}{\sqrt{\tilde{\omega}^2(\nu-z+i\delta) - \tilde{\Delta}^2(\nu-z+i\delta;\phi')}} \right\rangle' \\ &+ i\pi \Gamma^+ \frac{\Omega(\nu)}{c^2 + D^2(\nu) + \Omega^2(\nu)}. \end{aligned} \quad (1b)$$

In the above  $\tilde{\Delta}(i\omega_m;\phi)$  is the pairing energy evaluated at the fermionic Matsubara frequencies  $\omega_m = \pi T(2m-1)$ ,  $m$

$= 0, \pm 1, \pm 2, \dots$ . Here  $f(z)$  and  $n(z)$  are the Fermi and Bose distributions, respectively. The renormalized Matsubara frequencies are  $\tilde{\omega}(i\omega_m)$ . The analytic continuation to real frequency  $\nu$  of the above is  $\tilde{\Delta}(\nu+i\delta;\phi)$  and  $\tilde{\omega}(\omega+i\delta)$ , where  $\delta$  is a positive infinitesimal. The brackets  $\langle \dots \rangle$  are the angular average over  $\phi$ , and

$$\lambda(\nu) = \int_{-\infty}^{\infty} d\Omega \frac{I^2\chi(\omega)}{\nu - \Omega + i0^+}, \quad (2)$$

$$D(\nu) = \left\langle \frac{\tilde{\Delta}(\nu+i\delta;\phi)}{\sqrt{\tilde{\omega}^2(\nu+i\delta) - \tilde{\Delta}^2(\nu+i\delta;\phi)}} \right\rangle, \quad (3)$$

$$\Omega(\nu) = \left\langle \frac{\tilde{\omega}(\nu+i\delta)}{\sqrt{\tilde{\omega}^2(\nu+i\delta) - \tilde{\Delta}^2(\nu+i\delta;\phi)}} \right\rangle. \quad (4)$$

Equations (1) are a set of nonlinear coupled equations for the renormalized pairing potential  $\tilde{\Delta}(\nu+i\delta;\phi)$  and the renormalized frequencies  $\tilde{\omega}(\nu+i\delta)$  with the gap

$$\Delta(\nu+i\delta;\phi) = \frac{\tilde{\Delta}(\nu+i\delta;\phi)}{Z(\nu)}, \quad (5)$$

where the renormalization function  $Z(\nu)$  was introduced in the usual way as  $\tilde{\omega}(\nu+i\delta) = \nu Z(\nu)$ . In Eq. (1b),  $\Gamma^+$  sets the size of the impurity scattering and  $c$  is a parameter related to the impurity potential. The Born or weak scattering limit corresponds to a large value of  $c$  while the unitary or strong scattering limit corresponds to  $c=0$ . The impurity term is obtained from a  $T$ -matrix approach to the impurity problem.<sup>16</sup> It does not include all possible complications that have come to be known as possibly of some importance in the cuprates. Recent scanning tunneling microscopy (STM) data<sup>17,18</sup> has revealed significant inhomogeneities and impurity studies based on Bogoliubov-de Gennes (BdG) equations have shown that the superconducting order parameter is strongly modified in the vicinity of an impurity.<sup>19-27</sup> Such complications go well beyond the present approach. Here we will not attempt a complete microscopic description of the impurity scattering but instead treat  $\Gamma^+$  and  $c$  as parameters which we will determine through a best fit to data. To get a better fit may well require the introduction of more sophisticated effective potentials.

In the pure limit, i.e., no impurity contribution ( $\Gamma^+=0$ ), all parameters in Eqs. (1) that serve to characterize the particular material of interest are fixed from our previous work. The charge-carrier-fluctuation spectrum spectral density  $I^2\chi(\omega)$  which enters through Eq. (2) was previously obtained by Schachinger *et al.*<sup>5</sup> from infrared optical data using an inversion technique<sup>15</sup> which allows one to construct  $I^2\chi(\omega)$  from the optical scattering rate. In the present calculations we simply use these results without any modifications. The parameter  $g$  is also fixed and was determined to

get the measured value of the critical temperature in YBCO. While we will first present results in the clean limit we will later see that, to understand the low-temperature data ( $T \rightarrow 0$ ), we will need to consider some impurity scattering. The

value for  $\Gamma^+$  and  $c$  will be chosen to best fit the data as we have already emphasized.

The optical conductivity follows from knowledge of  $\tilde{\omega}$  and  $\tilde{\Delta}$ . The formula to be evaluated is

$$\begin{aligned} \sigma_{ab}(\Omega) = & \frac{i}{\Omega} \frac{e^2 N(0) v_F^2}{2} \left\langle \int_0^\infty d\nu \tanh\left(\frac{\nu}{2T}\right) \frac{1}{E(\nu; \phi) + E(\nu + \Omega; \phi)} [1 - N(\nu; \phi)N(\nu + \Omega; \phi) - P(\nu; \phi)P(\nu + \Omega; \phi)] \right. \\ & + \int_0^\infty d\nu \tanh\left(\frac{\nu + \Omega}{2T}\right) \frac{1}{E^*(\nu; \phi) + E^*(\nu + \Omega; \phi)} [1 - N^*(\nu; \phi)N^*(\nu + \Omega; \phi) - P^*(\nu; \phi)P^*(\nu + \Omega; \phi)] \\ & + \int_0^\infty d\nu \left[ \tanh\left(\frac{\nu + \Omega}{2T}\right) - \tanh\left(\frac{\nu}{2T}\right) \right] \frac{1}{E(\nu + \Omega; \phi) - E^*(\nu; \phi)} [1 + N^*(\nu; \phi)N(\nu + \Omega; \phi) \\ & + P^*(\nu; \phi)P(\nu + \Omega; \phi)] + \int_{-\Omega}^0 d\nu \tanh\left(\frac{\nu + \Omega}{2T}\right) \left\{ \frac{1}{E^*(\nu; \phi) + E^*(\nu + \Omega; \phi)} [1 - N^*(\nu; \phi)N^*(\nu + \Omega; \phi) \right. \\ & \left. - P^*(\nu; \phi)P^*(\nu + \Omega; \phi)] + \frac{1}{E(\nu + \Omega; \phi) - E^*(\nu; \phi)} [1 + N^*(\nu; \phi)N(\nu + \Omega; \phi) + P^*(\nu; \phi)P(\nu + \Omega; \phi)] \right\} \Bigg\rangle, \end{aligned} \quad (6a)$$

with

$$E(\omega; \phi) = \sqrt{\tilde{\omega}_{\mathbf{k}}^2(\omega) - \tilde{\Delta}_{\mathbf{k}}^2(\omega)} \quad (6b)$$

and

$$N(\omega; \phi) = \frac{\tilde{\omega}_{\mathbf{k}}(\omega)}{E(\omega; \phi)}, \quad P(\omega; \phi) = \frac{\tilde{\Delta}_{\mathbf{k}}(\omega)}{E(\omega; \phi)}. \quad (6c)$$

In the above,  $\langle \dots \rangle$  means, as before, an average over the angle  $\phi$  and the star refers to the complex conjugate.  $N(0)$  is the electronic density of states at the Fermi surface and  $v_F$  the Fermi velocity. The prefactor in Eq. (6a) can be worked out to be proportional to the plasma frequency squared,  $\Omega_p^2/4\pi \equiv n e^2/m^*$ . Here  $n$  is the electron density,  $e$  the electron charge, and  $m^*$  its effective mass.

### III. RESULTS AND DISCUSSION

In Fig. 1 which has five frames we show our results for the temperature dependence of the real part of the microwave conductivity  $\sigma_1(\omega)$  in the pure limit (open triangles), i.e.,  $\Gamma^+ = 0$  in Eq. (1), at the five measured frequencies of Hosseini *et al.*<sup>14</sup> They correspond from top frame to bottom frame to  $\Omega = 1.14, 2.25, 13.4, 22.7,$  and  $75.3$  GHz, respectively. For the lowest frequencies considered, the agreement with the data (solid squares), which we read off a graph in Ref. 11, is not good but the agreement does improve as the microwave frequency is increased. In particular, in the two top frames the height of the calculated peak is too high and it falls at a somewhat lower temperature than indicated in the measured curve. These deficiencies can be largely removed when a small amount of impurity scattering is additionally

included. The effect of impurity scattering will show up most prominently at the lowest temperature where the inelastic scattering is becoming very small.

Before proceeding with a fit to the data which includes both impurities and the inelastic scattering it is useful to first consider the BCS limit of our generalized Eliashberg equations (1) and to understand the effect of impurities in this instance. At low temperatures, the inelastic scattering rate which depends on real processes is small and the impurities will dominate; thus the BCS theory will become more applicable although it does ignore all renormalizations from the inelastic interaction (virtual processes).

To obtain the BCS equations from Eqs. (1) we ignore the effect of  $I^2\chi(\omega)$  in the renormalization channel, so

$$\tilde{\omega}(\nu + i\delta) = \nu + i\pi\Gamma^+ \frac{\Omega(\nu)}{c^2 + \Omega(\nu)^2}, \quad (7)$$

and in the gap channel we assume that the Boson frequency in  $I^2\chi(\omega)$  is very high compared with all other energies of importance. This means that Bose and Fermi factors in the second term on the right-hand side of Eq. (1a) are negligible and we can also replace the  $\lambda(\nu \pm i\omega_m)$  by a constant ( $\lambda$ ) with a cutoff ( $\omega_c$ ) on the Matsubara sum applied to get convergence. This gives a gap  $\tilde{\Delta}(\phi)$  independent of frequency  $\nu$  which satisfies the equation

$$\tilde{\Delta}(\phi) = 2\pi T g \cos(2\phi) \sum_{m=0}^{\omega_c} \lambda \left\langle \frac{\tilde{\Delta}(\phi') \cos(2\phi')}{\sqrt{\tilde{\omega}^2(i\omega_m) + \tilde{\Delta}^2(\phi')}} \right\rangle'. \quad (8)$$

The impurities enter directly in Eq. (7) and affect the gap given in Eq. (8) through the renormalized Matsubara frequency  $\tilde{\omega}(i\omega_m)$  which appears in the square root in the denominator. In the limit of  $\nu = 0$  we can write

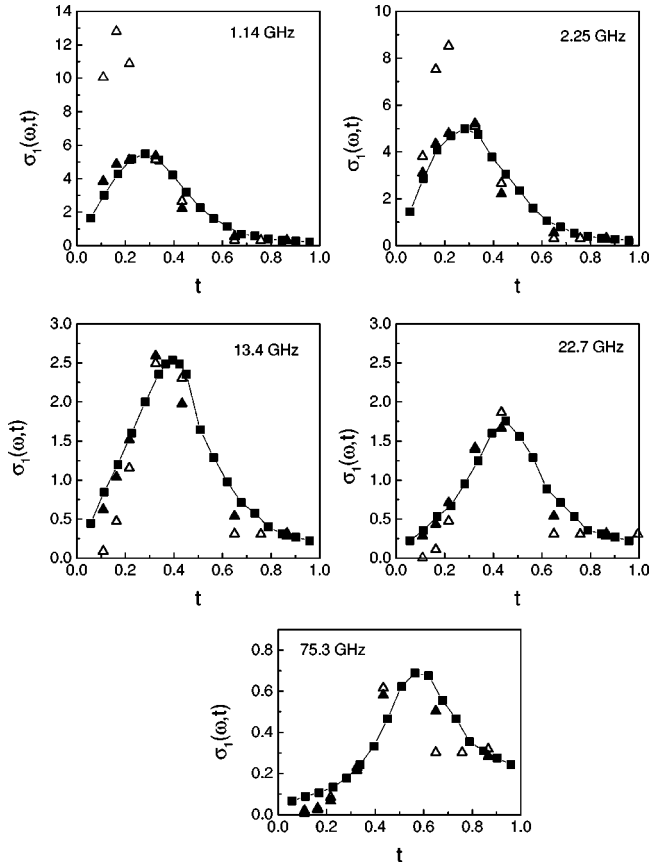


FIG. 1. Microwave conductivity  $\sigma_1(\omega, t)$  in  $10^7 \Omega^{-1} \text{ m}^{-1}$  vs the reduced temperature  $t = T/T_c$  for the five frequencies measured in experimental work of Hosseini *et al.* (Ref. 14), namely,  $\Omega = 1.14 \text{ GHz}$ ,  $2.25$ ,  $13.4$ ,  $22.7$ , and  $75.3 \text{ GHz}$  (bottom frame). Solid squares are experiment, open triangles clean limit, and solid triangles inelastic scattering plus impurities characterized by a potential with  $\Gamma^+ = 0.003 \text{ meV}$  and  $c = 0.2$ .

$$\tilde{\omega}(\nu + i\delta) \approx i\gamma \equiv i\pi\Gamma^+ \frac{\Omega(i\gamma)}{c^2 + \Omega(i\gamma)^2}, \quad (9)$$

which can be solved self-consistently for the impurity scattering rate at zero frequency. We can evaluate  $\Omega(\tilde{\omega}) = 2K(\Delta_0/\tilde{\omega})/\pi$  where  $K(x)$  is the elliptic integral of the first kind.<sup>28</sup> The quantity  $\Omega(i\gamma)$  appearing in Eq. (9) is  $\Omega(i\gamma) = [2\gamma/(\pi\Delta_0)] \ln(4\Delta_0/\gamma)$  and for a general value of  $c$ , the equation for  $\gamma$  is

$$\gamma = \pi\Gamma^+ \frac{\frac{2\gamma}{\pi\Delta_0} \ln\left(\frac{4\Delta_0}{\gamma}\right)}{c^2 + \left(\frac{2\gamma}{\pi\Delta_0}\right)^2 \ln^2\left(\frac{4\Delta_0}{\gamma}\right)}. \quad (10)$$

This equation shows that the self-consistent impurity scattering rate  $\gamma$  at zero frequency in the superconducting state is strongly dependent on the parameter  $c$ . For the strong-coupling unitary limit  $c=0$  an approximate solution has been given by Hirschfeld and Goldenfeld<sup>28</sup> for  $\pi\Gamma^+ \ll \Delta_0$  as

$$\gamma \approx 0.63 \sqrt{\pi\Gamma^+ \Delta_0}. \quad (11)$$

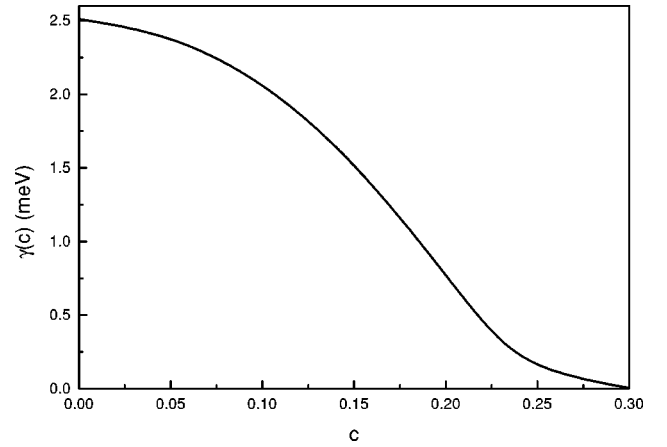


FIG. 2. The self-consistent impurity scattering rate  $\gamma(c)$  in the superconducting  $d$ -wave state given by Eq. (10) for various values of the impurity potential  $c$ . It is largest for  $c=0$  which corresponds to the unitary limit and rapidly becomes small as  $c$  increases beyond  $0.3$ . The corresponding normal scattering rate that we should compare  $\gamma(c)$  with is  $\pi\Gamma^+/(1+c^2)$ . Here  $\Gamma^+ = 0.15 \text{ meV}$  and  $\Delta_0 = 24\sqrt{2} \text{ meV}$ .

Note that  $\gamma(c=0)$  is much larger than  $\pi\Gamma^+$  in this limit. In the opposite limit (Born limit or weak-scattering potential)  $c \rightarrow \infty$  and  $\pi\Gamma^+/c^2$  is to be replaced by  $\pi\Gamma_N$  and

$$\gamma(c \rightarrow \infty) = 4\Delta_0 e^{-\Delta_0/(2\Gamma_N)}, \quad (12)$$

which shows that  $\gamma(c \rightarrow \infty)$  is now much smaller than the normal-state value of  $\Gamma$ ,  $\Gamma_N$ .

This analysis demonstrates that the zero-frequency self-consistent scattering rate in the superconducting state is much larger than its normal-state value in the unitary limit but is much smaller in the Born limit. In particular, this implies that in the Born limit the impurity-limited quasiparticle mean free path for a given impurity content will be much larger in the superconducting state than in the corresponding normal state if the inelastic scattering is ignored.

In Fig. 2 we illustrate the general case. What is plotted is  $\gamma(c)$  as a function of  $c$  for a specific value of  $\Gamma^+ = 0.15 \text{ meV}$  and a zero-temperature gap of  $\Delta_0 = 24\sqrt{2} \text{ meV}$ . The underlying normal-state scattering rate with which  $\gamma(c)$  is to be compared is  $\pi\Gamma^+/(1+c^2)$  for any value of  $c$ . In this example for  $c=0$ ,  $\gamma(c)$  is larger than  $\pi\Gamma^+$  (by a factor of 5), for  $c=0.2$  they are comparable, and for  $c=0.3$  it is already much less. By changing  $c$  we can change the value of quasiparticle scattering rate at  $\nu=0$  in the superconducting state by orders of magnitude and this will be of importance for our analysis of the experimental data.

It is instructive to look as well at the frequency dependence of the underlying quasiparticle scattering rate or, more precisely, the imaginary part of the renormalized frequency, namely,

$$\tau^{-1}(\nu) = \text{Im}\tilde{\omega}(\nu) = \tilde{\omega}_2(\nu) = \pi\Gamma^+ \frac{\Omega[\tilde{\omega}(\nu)]}{c^2 + \Omega^2[\tilde{\omega}(\nu)]}. \quad (13)$$



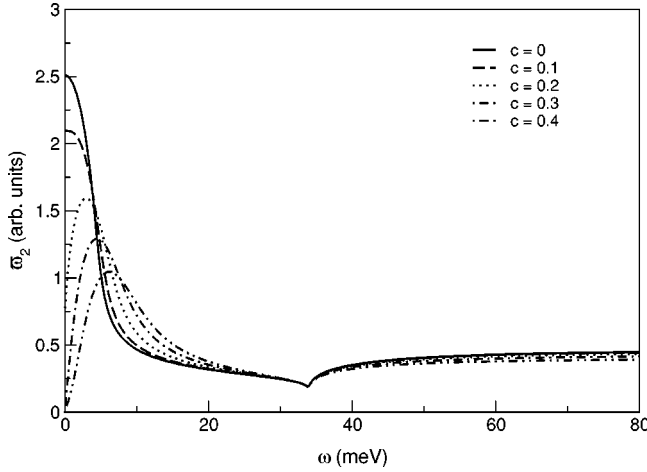


FIG. 3. The imaginary part of the renormalized frequency  $\tilde{\omega}_2(\nu)$  as a function of  $\nu$  for several values of the impurity parameter  $c$ , namely,  $c=0$  (solid line),  $c=0.1$  (dashed line),  $c=0.2$  (dotted line),  $c=0.3$  (dash-dotted line), and  $c=0.4$  (dash-double-dotted line). Here  $\Gamma^+=0.15$  meV and  $\Delta_0=24\sqrt{2}$  meV.

In Fig. 3 we show results for several values of  $c$ . The behavior of  $\tau^{-1}(\nu)$  versus  $\nu$  at small  $\nu$  changes radically with choice of  $c$ . In the unitary limit there is a small region where  $\tau^{-1}(\nu)$  is fairly flat, but for finite  $c$ ,  $\tau^{-1}(\nu)$  begins to look like a  $d$ -wave quasiparticle density of states and the scattering is radically affected by the onset of superconductivity which modifies the density of final states available for scattering. These effects can be understood simply in the clean limit  $\Gamma^+\rightarrow 0$  and for temperatures  $T>\gamma$ . This limit is considered in the work of Hirschfeld *et al.*<sup>29</sup> who treat the two cases  $c=0$  and  $c\rightarrow\infty$  explicitly. Here we consider finite  $c$  and  $\nu$  small ( $\ll\Delta_0$ ),<sup>30</sup>

$$\tau^{-1}(\nu) = \pi\Gamma^+ \frac{\nu}{\Delta_0} \frac{c^2 + A_+(\nu)}{c^4 + 2c^2 A_-(\nu) + (4\nu/\Delta_0)^2 A_+(\nu)}, \quad (14)$$

with

$$A_{\pm}(\nu) = \left(\frac{4\nu}{\Delta_0}\right)^2 \left[ \left(\frac{\pi}{2}\right)^2 \pm \ln^2\left(\frac{2\Delta_0}{\omega}\right) \right]. \quad (15)$$

It is clear that for  $c\rightarrow\infty$   $\tau^{-1}(\nu)$  becomes proportional to  $\nu$  while for  $c=0$  it goes like  $\nu^{-1}$  at small  $\nu$ . For a general  $c$ , the quasiparticle scattering rate  $\tau^{-1}(\nu)$  is importantly dependent on  $\nu$  and, therefore, is quite different for the constant of the familiar normal-state Drude model. This means that, while we have two parameters  $\Gamma^+$  and  $c$  to adjust, the underlying complicated variation of  $\tau^{-1}(\nu)$  with  $\nu$  gets reflected directly in the frequency variation of the conductivity and leads to a non-Drude form in sharp contrast to the underlying normal state.

We present results in Fig. 4. What is plotted is the real part of the conductivity  $\sigma_1(\omega, T)$  in units of  $N(0)v_F^2$  as a function of frequency  $\omega$  in the range up to 1.0 meV ( $\sim 242$  GHz). The temperature is set at  $T=10$  K and the impurity scattering at  $\Gamma^+=0.15$  meV in Eq. (7). Various values of the impurity parameter  $c$  are shown. The solid gray

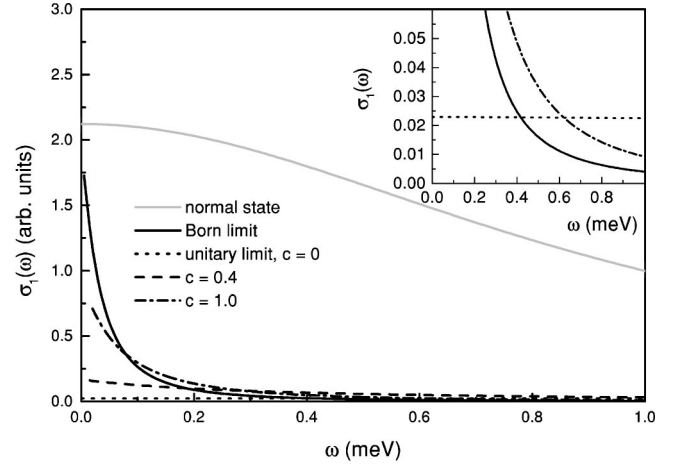


FIG. 4. The real part of the optical conductivity  $\sigma_1(\omega)$  in BCS theory with  $\Gamma^+=0.15$  meV at temperature  $T=10$  K for various values of the impurity parameter  $c$ , namely, Born limit ( $c\rightarrow\infty$ , solid line), unitary limit ( $c=0$ , dotted line),  $c=0.4$  (dashed line), and  $c=1.0$  (dash-dotted line). The solid gray curve is for comparison and gives the normal state. The inset shows the same results on a different vertical scale.

curve in Fig. 4 is the normal state shown for comparison. It displays the classical Drude form with a Drude width of  $\pi\Gamma^+$ . The other curves are in the superconducting state at  $T=10$  K with the zero-temperature  $d$ -wave gap taken to be  $\Delta_0=24\sqrt{2}$  meV. The black solid curve is the Born limit, dotted the unitary limit, dashed  $c=0.4$ , and dash-dotted  $c=1.0$ . None of the curves in the superconducting state follow the Drude form of the normal state,  $\sigma_1(\omega) = 2\tau_{imp}/[1 + (\omega\tau_{imp})^2]$ , with  $\tau_{imp}=2.12$  meV<sup>-1</sup>. The curves near the Born limit show a concave up rather than the concave down behavior of the normal-state Drude model. The curve for the unitary limit is much flatter than the solid gray curve reflecting a value of  $\gamma(c)$  which is large compared with its normal-state counterpart. The inset in the top right-hand side shows this on a different scale and allows the reader to better see the radical difference in behavior between the Born and unitary limits. Although neither of these limits show a Drude variation with  $\omega$ , we can still think of the half width of each curve as giving a measure of the underlying quasiparticle scattering rate. One then concludes that in the Born limit it is much smaller than in the normal state while in the unitary limit it is much larger.

The data in the work of Hosseini *et al.*<sup>14</sup> which we use here for comparison with theory were fit to a Drude form and the authors concluded that the effective quasiparticle scattering rate was fairly temperature independent and constant. It is clear from our Eq. (14) and Fig. 3 that this behavior will never be reproduced in a BCS theory with only elastic impurity scattering whatever the value of  $c$ . The underlying quasiparticle scattering rates are always highly frequency dependent and this modulates the Drude linewidth as  $\omega$  changes. This also implies a temperature dependence since a change in  $T$  involves a different sampling of the frequency dependence of  $\tau^{-1}(\omega)$ . Any two-fluid approach would need to account for these features of the scattering rates of the

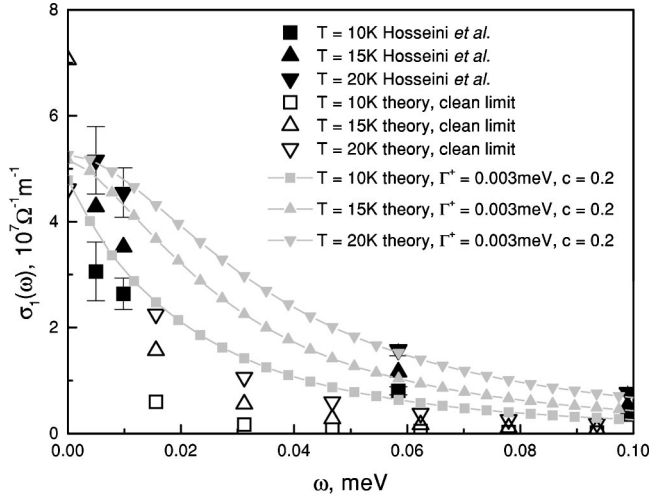


FIG. 5. The microwave conductivity  $\sigma_1(\omega, T)$  as a function of  $\omega$  for three different temperatures. The data are the same as shown in Fig. 1. The open symbols are theory for the pure limit, the solid gray symbols theory with some impurity scattering additionally included, and the solid black symbols are experiments. The squares are for  $T=10$  K, the upward triangles for  $T=15$  K, and the down triangles for  $T=20$  K.

normal quasiparticles as well as the energy dependence in the density of states.<sup>29</sup> Including some impurity scattering in addition to the inelastic scattering in Eq. (1) greatly improves the agreement with experiment. The half width of the conductivity as a function of  $\omega$  in our clean-limit Eliashberg calculations is significantly smaller than what is observed experimentally. (See Fig. 5, open symbols.) This does allow us to add some impurities which of course always result in an increase of the half width.

To make an appropriate choice of  $\Gamma^+$  and of  $c$  we are guided by the Drude analysis of the data provided by Hosseini *et al.*<sup>14</sup> They find a very narrow width to their Drude form of the order of 1/3 K. It is clear that the amount of impurities involved is very small and that  $\pi\Gamma^+/(1+c^2) = \gamma_N(c)$ , which gives the scattering in the normal state, is correspondingly small. It is also clear that the unitary limit is unlikely since this increases  $\gamma(c)$  considerably as compared with the normal-state equivalent  $\gamma_N(c)$  which would then have to be much smaller than 1/3 K which is not likely. On the other hand, the Born limit gives a concave upward curve which drops too rapidly as  $\omega$  increases out of zero. It appears that some intermediate  $c$  value is favored but on examination of Fig. 3 and the form (14) it is clear that our best fit still differs from the Drude form for conductivity.

After some trial and error we came up with  $\Gamma^+ = 0.003$  meV and  $c=0.2$ . Our new results which include inelastic as well as impurity scattering are shown as the solid triangles in Fig. 1. The agreement with the data is clearly greatly improved over the pure limit, i.e.,  $\Gamma^+=0$ , in Eq. (1), particularly at low temperatures and for the smaller microwave frequencies used in the experiment. The over all fit to the entire data set is quite good but certainly not excellent. The theoretical calculations do reproduce well the general trends such as the decrease in peak height with increasing

microwave frequency and its shift to higher energies. The inelastic scattering largely controls this trend and the present analysis provides support for the validity of the charge-carrier-fluctuation spectrum spectral weight  $I^2\chi(\omega)$  used here. We stress that the form of  $I^2\chi(\omega)$  was not adjusted in any way to fit the microwave data but comes from consideration of the infrared optical scattering rate only.

One can further examine the quality of the fit by plotting the same data as a function of frequency for fixed temperature  $T$ . This is done in Fig. 5. In the figure the black solid symbols are experiment, gray solid symbols theory with impurities ( $\Gamma^+=0.003$  meV,  $c=0.2$ ), and the open symbols the pure case, i.e., including only the inelastic scattering captured in our model spectral density  $I^2\chi(\omega)$ . It is quite clear that some impurity scattering is needed to get even reasonably close to the data although a tight fit is never possible. The data do not vary as rapidly at the lowest frequency values as in theory. We point out, however, that the fit is very much better than we could achieve using a pure BCS formalism. Inclusion of inelastic scattering is essential in any serious attempt to understand these data even at reasonably low temperatures. Our use of the generalized Eliashberg equations, given in the previous section, can be viewed as a phenomenology with kernel  $I^2\chi(\omega)$  determined from experimental data. We have previously found that this phenomenology is able to explain many of the anomalous superconducting properties observed in the oxides. The present study extends the range of agreement to the microwave data although some discrepancies do remain. These are not large, however. In Fig. 5 the data for 20 K fit perfectly, for 10 K we have only disagreement for 1 GHz, and at 15 K we have a slight disagreement for 1 and 2 GHz. But for these two temperatures Hosseini *et al.*<sup>14</sup> also have problems with their Drude fits. The overall fit seems to be as good as the one of Hosseini *et al.*<sup>14</sup> and also as in the analysis of Berlinisky *et al.*<sup>31</sup> who conclude that the data do not support a quasiparticle picture. Here we find, instead, no serious disagreement of the data with an Eliashberg formulation of the  $d$ -wave state which includes some impurity scattering described with an intermediate value of  $c$ , the parameter that spans the interaction strength from the unitary ( $c=0$ ) to the Born ( $c=\infty$ ) limit.

#### IV. CONCLUSION

We have made use of a set of charge carrier-boson exchange spectral densities  $I^2\chi(\omega)$  obtained previously from an analysis of infrared optical conductivity data to calculate the microwave conductivity at several frequencies as a function of temperature in a generalized Eliashberg formalism suitable to describe a  $d$ -wave superconductor. Agreement with recent data on pure samples of  $\text{YBa}_2\text{Cu}_3\text{O}_{6.99}$  is satisfactory provided a small amount of elastic impurity scattering is also included. The impurity potential used is neither in the Born (weak) nor unitary (strong) limit. A potential of intermediate strength is indicated. The low-temperature behavior found in the theory cannot accurately be described by a Drude form and does not support the use of a two-fluid model with the normal component described by a scattering

rate constant in frequency although temperature dependent. Instead, the conductivity as a function of energy at fixed  $T$  is concave upward reflecting the intrinsic frequency dependence of the combined scattering rates. This holds even when inelastic scattering is included. The calculations show clearly that, in the main, the main features of the microwave data can be understood within the same generalized Eliashberg formalism that has recently been so successful in describing many of the anomalous superconducting-state properties<sup>5</sup> seen in the oxides. This follows also from the observation by Schachinger and Carbotte<sup>32</sup> that adding elastic impurity scattering only affects the low-energy region of the optical prop-

erties while the inelastic scattering effects are seen in the energy region  $\omega > \Delta_0$ . Thus, adding elastic impurity scattering allows a fit of theoretical Eliashberg results to match the low-energy optical properties of a particular sample without violating all earlier findings which particularly concentrated on the energy region  $\omega > \Delta_0$  or on bulk effects.

#### ACKNOWLEDGMENTS

This research was supported by the Natural Sciences and Engineering Research Council of Canada (NSERC) and by the Canadian Institute for Advanced Research (CIAR).

- 
- <sup>1</sup>J.P. Carbotte, E. Schachinger, and D.N. Basov, *Nature* (London) **401**, 354 (1999).
- <sup>2</sup>Ph. Bourges, Y. Sidis, H.F. Fong, B. Keimer, L.P. Regnault, J. Bossy, A.S. Ivanov, D.L. Milius, and I.A. Aksay, in *High Temperature Superconductivity*, edited by S. E. Barnes *et al.* (American Institute of Physics, Amsterdam, 1999), pp. 207–212.
- <sup>3</sup>E. Schachinger and J.P. Carbotte, *Phys. Rev. B* **62**, 9054 (2000).
- <sup>4</sup>E. Schachinger and J.P. Carbotte, *Physica C* **341-348**, 79-82 (2000).
- <sup>5</sup>E. Schachinger, J.P. Carbotte, and D.N. Basov, *Europhys. Lett.* **54**, 380 (2001).
- <sup>6</sup>E. Schachinger, J.P. Carbotte, and F. Marsiglio, *Phys. Rev. B* **56**, 2738 (1997); **57**, 7970 (1998).
- <sup>7</sup>A.J. Millis, H. Monien, and D. Pines, *Phys. Rev. B* **42**, 167 (1990).
- <sup>8</sup>P. Monthoux and D. Pines, *Phys. Rev. B* **47**, 6069 (1993).
- <sup>9</sup>P. Dai, H.A. Mook, S.M. Hayden, G. Aeppli, T.G. Perring, R.D. Hunt, and F. Doğan, *Science* **284**, 1344 (1999).
- <sup>10</sup>M.C. Nuss, P.M. Mankiewich, N.L. O'Malley, and E.H. Westwick, *Phys. Rev. Lett.* **66**, 3305 (1991).
- <sup>11</sup>D.A. Bonn, R. Liang, T.M. Risemann, D.J. Baar, D.C. Morgan, K. Zhang, P. Dosanjh, T.L. Duty, A. McFarlane, G.D. Morris, J.H. Brewer, W.N. Hardy, C. Kallin, and A.J. Berlinsky, *Phys. Rev. B* **47**, 11 314 (1993).
- <sup>12</sup>M. Matsukawa, T. Mizukoshi, K. Noto, and Y. Shiohara, *Phys. Rev. B* **53**, R6034 (1996).
- <sup>13</sup>H.-Y. Kee, S.A. Kivelson, and G. Aeppli, *cond-mat/0110478* (unpublished).
- <sup>14</sup>A. Hosseini, R. Harris, S. Kamal, P. Dosanjh, J. Preston, R. Liang, W.N. Hardy, and D.A. Bonn, *Phys. Rev. B* **60**, 1349 (1999).
- <sup>15</sup>F. Marsiglio, T. Startseva, and J.P. Carbotte, *Phys. Lett. A* **245**, 172 (1998).
- <sup>16</sup>M. Prohammer and J.P. Carbotte, *Phys. Rev. B* **43**, 5370 (1991).
- <sup>17</sup>S.H. Pan, E.W. Hudson, K.M. Lang, H. Eisaki, S. Uchida, and J.C. Davis, *Nature* (London) **403**, 746 (2000).
- <sup>18</sup>E.W. Hudson, S.H. Pan, A.K. Gupta, K.-W. Ng, and J.C. Davis, *Science* **285**, 88 (1999).
- <sup>19</sup>M. Franz, C. Kallin, A.J. Berlinsky, and M.I. Salkola, *Phys. Rev. B* **56**, 7882 (1997).
- <sup>20</sup>A. Ghosal, M. Randeria, and N. Trivedi, *cond-mat/0004481* (unpublished).
- <sup>21</sup>M. Franz, C. Kallin, and A.J. Berlinsky, *Phys. Rev. B* **54**, R6897 (1996).
- <sup>22</sup>J.-X. Zhu, C.S. Ting, and Chia-Ren Hu, *Phys. Rev. B* **62**, 6027 (2000).
- <sup>23</sup>W.A. Atkinson, P.J. Hirschfeld, and A.H. MacDonald, *Phys. Rev. Lett.* **85**, 3922 (2000).
- <sup>24</sup>W.A. Atkinson, P.J. Hirschfeld, A.H. MacDonald, and K. Ziegler, *Phys. Rev. Lett.* **85**, 3926 (2000).
- <sup>25</sup>A.V. Balatsky, M.I. Salkola, and A. Rosengren, *Phys. Rev. B* **51**, 15 547 (1995).
- <sup>26</sup>M.I. Salkola, A.V. Balatsky, and D.J. Scalapino, *Phys. Rev. Lett.* **77**, 1841 (1996).
- <sup>27</sup>J.-X. Zhu and C.S. Teng, *Phys. Rev. B* **63**, 020506 (2001).
- <sup>28</sup>P.J. Hirschfeld and N. Goldenfeld, *Phys. Rev. B* **48**, 4219 (1993).
- <sup>29</sup>P.J. Hirschfeld, W.D. Putika, and D. Scalapino, *Phys. Rev. B* **50**, 10 250 (1994).
- <sup>30</sup>Wen Chin Wu helped with the derivation of this result.
- <sup>31</sup>A.J. Berlinsky, D.A. Bonn, R. Harris, and C. Kallin, *Phys. Rev. B* **61**, 9088 (2000).
- <sup>32</sup>E. Schachinger and J.P. Carbotte, *Phys. Rev. B* **64**, 094501 (2001).